EFFECT OF SHEAR STRAIN ON DEFORMED MICROSTRUCTURES OF AUSTENITIC GRAINS

Tadanobu Inoue, Fuxing Yin and Kotobu Nagai
Steel Research Center, National Institute for Materials Science, Japan

ABSTRUCT

Electron backscattered diffraction analysis is used to investigate the effect of shear deformation on the microstructural evolution of a Ni-30Fe alloy during hot deformation. An explicit finite element analysis was carried out to evaluate the inhomogeneous strain distribution introduced in the specimens by hot compression simulator. The deformation structures in no shear strain area are compared with these in shear strain area under the same equivalent strain. The fraction of high angle grain boundaries (HAGBs) having misorientations in excess of 15^o increased with an increase in equivalent strain. Such the expense occurred at much higher rate with shear strain than without shear strain. The shear strain component is more effective to develop HAGBs in austenite grain interiors than the compressive strain.

KEYWORDS

Nickel-30 ferrous alloy, Microstructural evolution, Misorientation angle, Shear strain, Strain components

INTRODUCTION

The plastic strain is generally composed of two strain components or has two deformation modes: shear strain and the compressive (or tensile) strain. It is expected that these two strain components coexist in the materials deformed by the heavy deformation techniques. The shear strain is known to be more effective for creating finer ferrite grains than the compressive strain due to the faster increasing rate of austenite grain boundary surface area per unit volume[1]. Recently, Inoue *et al*. have reported that under the same equivalent strain ε_{eq}, the ferrite grain size in the area with the shear strain is finer than that in the area without the shear strain[2-3]. At the same time it is also expected that the different type of plastic strain will introduce significant changes in the microstructural evolution behavior of austenite grain interiors. In this study, the effect of deformation mode on the microstructural evolution of Ni-30Fe alloy hot compressed by a pair of anvils is investigated. The explicit FE-analysis is used to evaluate the inhomogeneous strain distribution in the specimens compressed by reduction ratios of 50% and 75%. On the basis of the calculated strain distribution, the microstructural evolution behaviors in the positions with and without the shear strain γ_{xy} are compared according to the equivalent strain ε_{eq}. The effect of the shear strain on the microstructural evolution is investigated in the range of $0 \leq \gamma_{xy} \leq 2.29$ at the fixed ε_{eq} of 1.5 by means of EBSD technique.

1. EXPERIMENTAL PROCEDURE

The ingot of Ni-30Fe alloy (0.002C-0.008Si- 69.8Ni) was prepared in a vacuum induction melting furnace with a weight capacity of 50kg. The ingot was re-heated to 1473K and hot rolled to make a plate with a size of $60t \times 140w \times 550L$ (mm). The final rolling temperature was 1243K. Rectangular specimens that were 12mm in thickness, 20mm in width and 18mm in length were machined from the hot rolled plate for hot compression test. A hot compression simulator was used for the thermo-mechanical treatment. The specimen was heated to 1023K and held for 20 seconds and then deformed by reduction ratios of 50% and 75% at a strain rate of 1/s. The deformation temperature of 1023K was known to be in non-recrystallized region[4]. The deformed specimen was quenched to room temperature by water jet immediately after the compression. The specimen surface observed was parallel to the compression direction, as shown in Fig. 1. The microstructures were characterized by optical microscopy and scanning electron microscopy. The grain orientations were determined by scanning electron microscopy (LEO Gemini 1550) using the TSL EBSD system. Low angle grain boundaries (LAGBs), or subgrain boundaries, were defined as boundaries with misorientation between 1.5° and 15° misorientation, and high angle grain boundaries (HAGBs), or grain boundaries, are defined as boundaries greater than 15° in the misorientation.

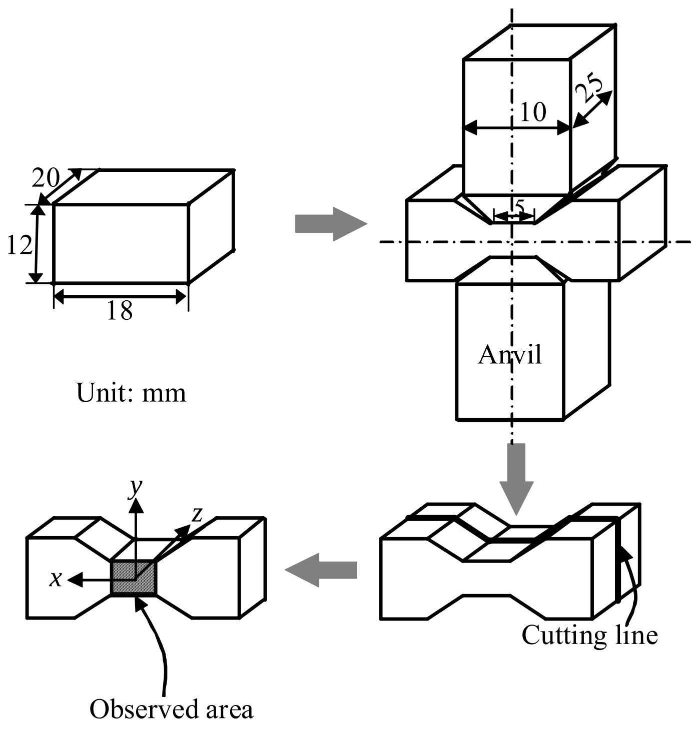

Fig. 1 Schematic drawing of compression test and observed area of deformed specimen

2. NUMERICAL ANALYSIS

The three-dimensional dynamic finite element simulation was carried out using the explicit FE-code ABAQUS/Explicit. The specimen is assumed to be isotropic and homogeneous. The anvil is regarded as a rigid body and the specimen is not constrained in the *x*-direction. An 8-node linear element was used for the specimen. And the finite element mesh in the sample includes 6552 nodes and 5400 elements. Furthermore, adaptive meshing was carried out in the analysis because the mesh becomes too degenerate on heavy deformation. The stress-strain relationships depending on a strain rate and temperature employed in the analysis were measured experimentally by compression test using a cylindrical specimen[2]. In the analysis, the Coulomb condition with a friction coefficient of 0.3 is used as the frictional condition on the contacting planes between the anvil and the specimen[2-3].

3. RESULTS AND DISCUSSION

3.1 PLASTIC STRAIN DISTRIBUTION AND MATERIAL FLOW

Figure 2 represents the contour maps showing the distributions of shear strain γ_{xy} and equivalent strain ε_{eq} after 50% and 75% reductions at 1023K and a strain rate of 1/s. The numerical analysis was carried out on the *x*-*y* plane of the gray quarter part of the specimen. As can be seen in Fig. 2, the γ_{xy} increases towards the anvil edge from the center and becomes zero along the *x* and *y* axes, which means that the plastic strains along the *x*- and *y*- direction show a plane strain condition, i.e., $\varepsilon_{xx}+\varepsilon_{yy}=0$, $\varepsilon_{zz}=0$. The ε_{eq} shows the maximum value at the specimen center and the anvil edges. The high compressive strains at the center and the high shear strains at the anvil edges seem to be responsible for the maximum equivalent strain.

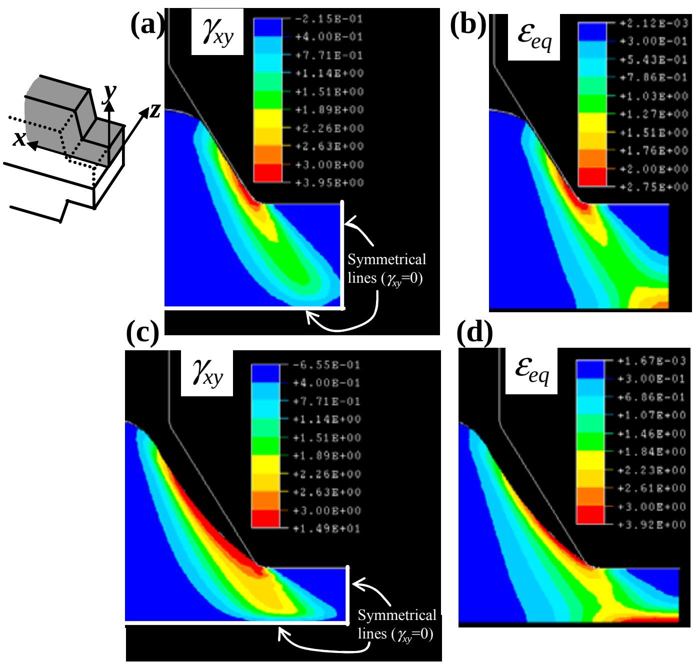

Fig. 2 Contour maps of (a) shear strain γ_{xy} and (b) equivalent strain ε_{eq} after 50% compression and (c) γ_{xy} and (d) ε_{eq} after 75% compression at 1023K and strain rate of 1/s

HOME

Microstructures at different sites on the cross- section surface of the 75% compressed specimen and contour map of ε_{eq} are shown in Fig. 3. The material flow toward anvil edges from center agrees with the region introduced a large equivalent strain. The microstructure below the contacting surface with anvils shows non-deformed austenite grains of about 90μm in diameter. Figures 3(b)-(d) show the magnified optical micrographs. They show different deformed microstructures from site to site. The difference in the deformed microstructures is due to the strain variation induced by hot compression, as seen in Fig. 2(c), (d).

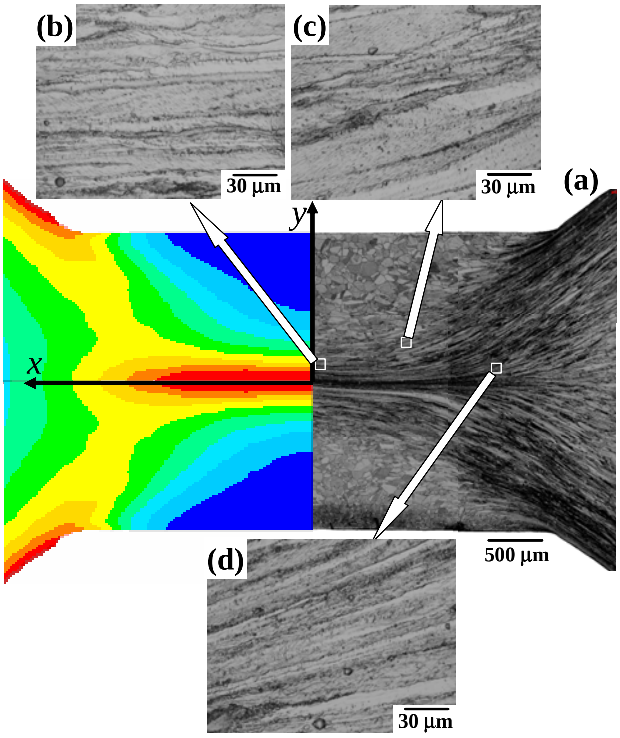

Fig. 3 (a) Optical micrograph (the right hand) and contour map of equivalent strain (the left side) after 75% compression and (b)-(d) magnified views of areas indicated by squares in (a)

3.2 EVOLUTION OF DEFORMED STRUCTURE WITH STRAIN

Figure 4 presents the EBSD maps of the deformed specimens by three equivalent strains without or with shear strain. The left hand side corresponds to the area along the y axis of Fig. 3(a), showing a plane strain compression without shear strain. On the other hand, the right hand side corresponds to the sites with shear strain γ_{xy} of 1.0. It can be seen that at ε_{eq} of 0.68 (Fig. 4(a), (b)), both deformed structures within austenite grains are composed of only LAGBs. At ε_{eq} of 1.70 (Fig. 4(c), (d)), the laminar elongation of the structure aligned in the material flow direction becomes more evident. New HAGBs were generated by the formation of deformation bands within austenite grains, signifying localized non- homogeneous deformation. With increasing ε_{eq} to 2.83 (Fig. 4(e), (f)), the grains are subdivided more rapidly by the formation of HAGBs in almost all the austenite grains.

In order to investigate the effect of shear strain component on the microstructural evolution, EBSD maps was determined for the sites with shear strain γ_{xy} up to 2.29, under the same equivalent strain ε_{eq} of 1.5 as shown in Fig. 5. With fixing the equivalent plastic strain at 1.5, the amount of compressive strain decreases with increasing shear strain. Since it becomes difficult to discern the austenite grain boundaries with increasing strain, SEM micrographs are also shown in Fig. 5. It can be seen that the site with a shear strain γ_{xy} of 0, that is, deformed with just compressive strain, new HAGBs were generated by the formation of deformation bands within austenite grains, as indicated by arrows. After deformation with shear strain of 1.92, some grains, indicated by arrows, were filled with fine HAGBs. With increasing the shear strain to 2.29, new HAGBs get developing on a much finer scale within almost all the austenite grains. From Fig. 5, it can be also known that the compressive direction varies with shear strain, contrary to no rotation of compressive direction in the sites without it. In order to express local strain, it is convenient to introduce a local coordinate system (1-2-3) whose axes coincide with the directions of the principal strains ε_1, ε_2 and ε_3 ($\varepsilon_1<\varepsilon_2<\varepsilon_3$). Using each strain value obtained in the specimen coordinate system (*x*-*y*-*z*), the directions of the principal axes in the local coordinate system and the principal strains are calculated. The schematic drawings of the principal axes (1-3) and the rotation angle ϕ from the *x* and *y* axes to the principal axes at each site are also illustrated in Fig. 5.

Under the same equivalent strain of 1.5, the principal strains at each site are almost identical around 1.2 with different shear strains from 0 to 2.29. Accordingly the deformed austenite grains have a similar thickness of approximately 25 μm as indicated by arrows in SEM micrographs of Fig. 5.

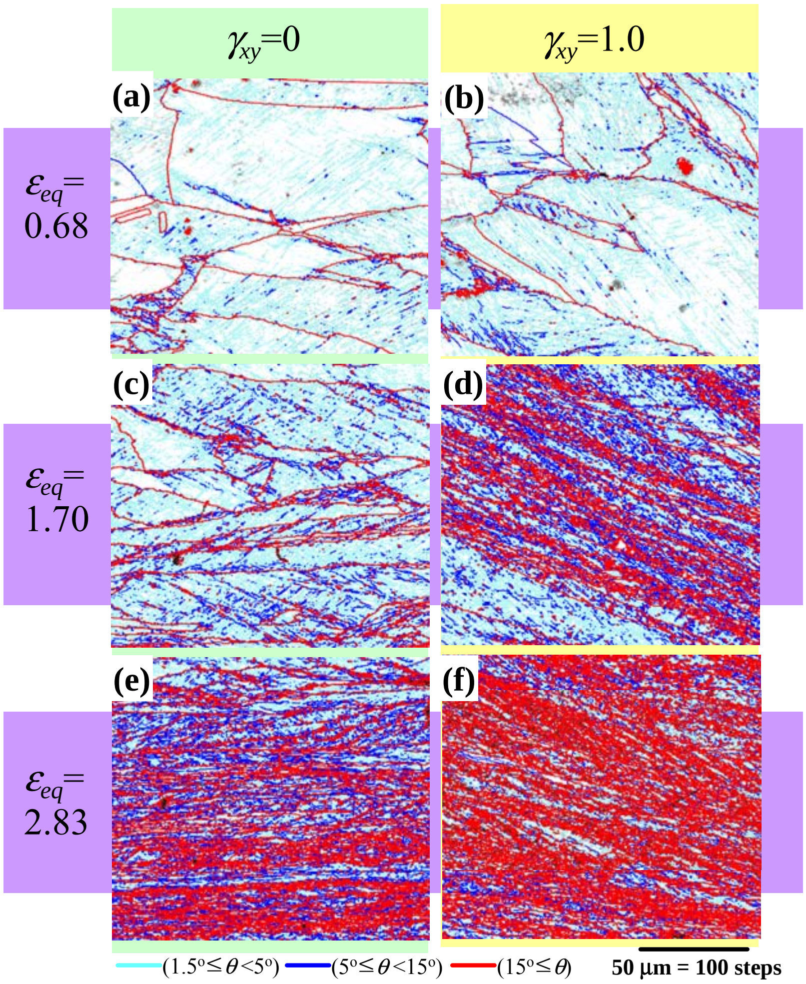

Fig. 4 EBSD maps showing the development of deformation structures according to equivalent strains (a), (b) ε_{eq}=0.68 (c), (d) ε_{eq}=1.70 and (e), (f) ε_{eq}=2.83; in (a), (c) and (e) no shear strain; in (b), (d) and (f) shear strain γ_{xy} of 1.0

HOME

On the other hand, the rotation angle ϕ calculated with shear strain becomes larger with increasing shear strain. For example, the rotation angle is 10° at the shear strain of 1.08 and 46° at the shear strain of 2.29. And further it shows a good agreement with the slope of the deformed austenite grain boundary when the SEM micrograph and the illustration of rotation angle in Fig. 5 are compared. These results imply that the compressive direction rotates continuously during deformation and a kind of multidirectional deformation occurs with an increase in shear strain. Multidirectional deformation is well known to be effective for grain refinement. That is, the multidirectional deformation is believed to induce multiplication of slip systems and enhance the formation of high

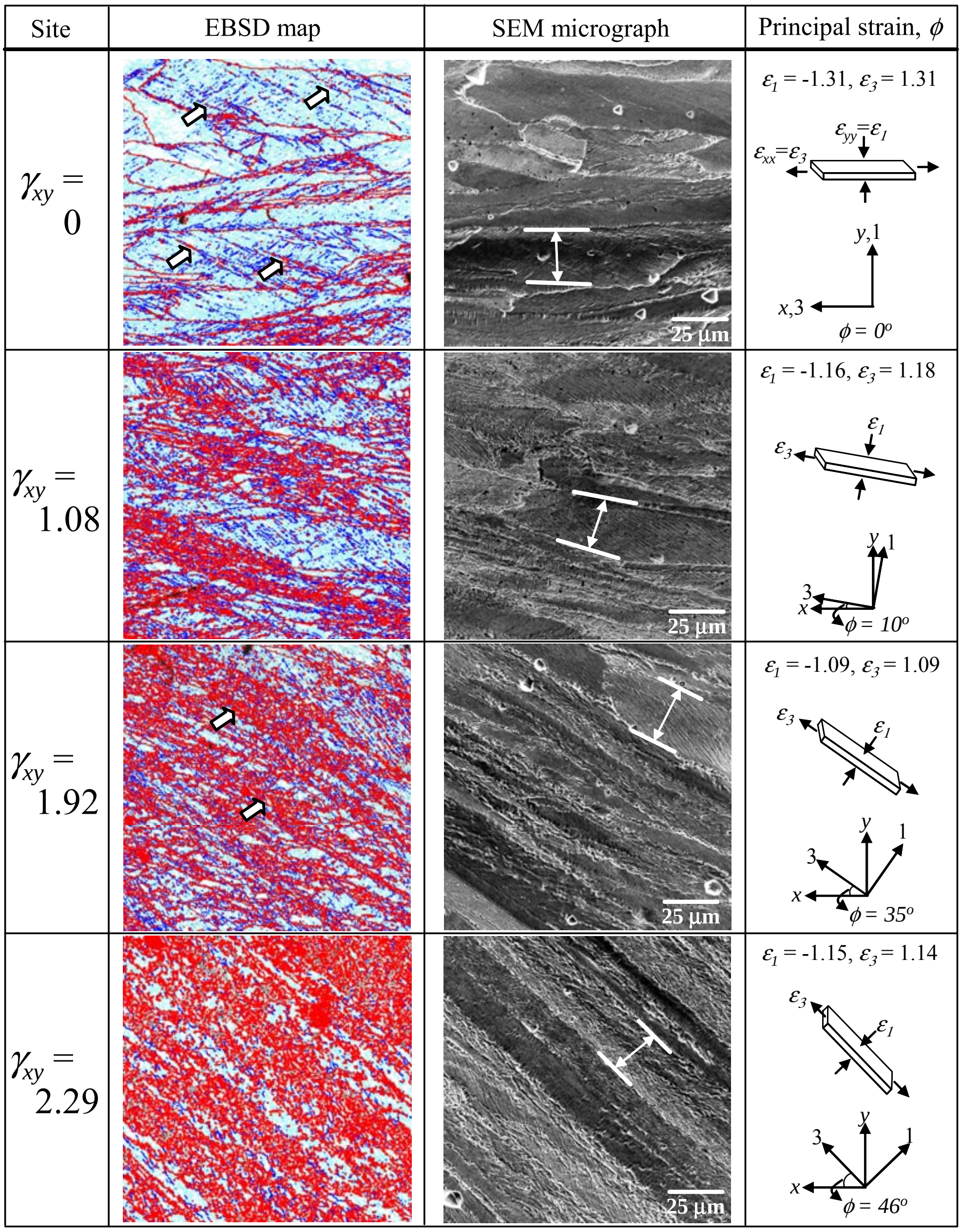

Fig. 5 EBSD maps, SEM micrographs and principal strains for some sites of shear strain γ_{xy} variable at equivalent strain of ε_{eq}=1.5. Here, ϕ means the rotation angle from x, y axes to principal axes

HOME

angle grain boundaries or the subdivision of grains. Consequently, even under the same equivalent strain, the increasing the shear strain might accelerate the subdivision of austenite grain interiors with increased misorientations between subdivided local areas.

3.3 STARISRICAL MEASUREMENTS OF THE MICROSTRUCTURAL EVOLUTION DURING DEFORMATION

The fractions of HAGB area are displayed as a function of equivalent strain ε_{eq} in Fig. 6. Figure 6 shows that the fraction of HAGB increases as ε_{eq} increases. And the existence of shear strain γ_{xy} makes the higher increase rate of increase in HAGB area fraction than no shear strain. At ε_{eq}=2.83, the fraction of HAGB is over 50% with γ_{xy} of 1.0, in comparison with only 30% without γ_{xy}. Even with the increased ε_{eq} of 3.5, the fraction of HAGB is still 43% HAGB without γ_{xy}. The typical boundary misorientation distribution determined from the EBSD maps is shown in Fig. 7 at an equivalent strain of 2.83 with and without shear strain. The graphs show the relative frequency of boundary misorientations at intervals of 3°. Misorientations less than 1.5° are omitted due to the orientation noise in EBSD measurements. The fraction of misorientation angle, especially between 30° and 50°, is approximately two times with shear strain as large as without shear strain. Figure 8 compares the rates of development of boundaries for each misorientation range with increasing equivalent strain in the area with and without shear strain component during deformation. In the graphs two classes of HAGBs are shown; lower high angle grain boundaries with misorientations between 15° and 30°, and very high angle grain boundaries with misorientations in

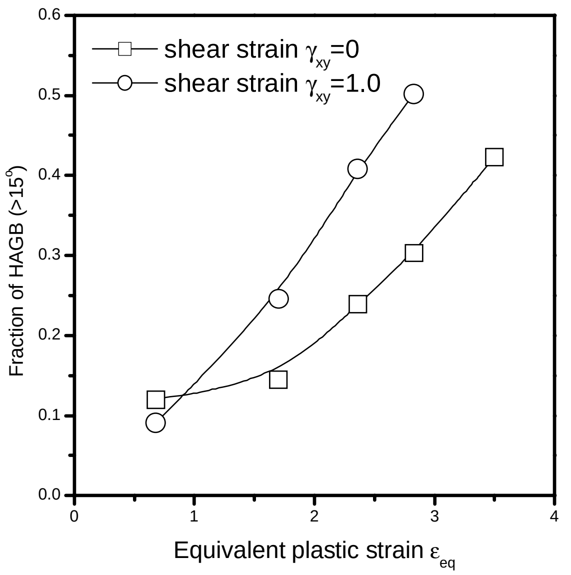

Fig. 6 Fraction of HAGB area plotted as a function of equivalent plastic strain with and without shear strain

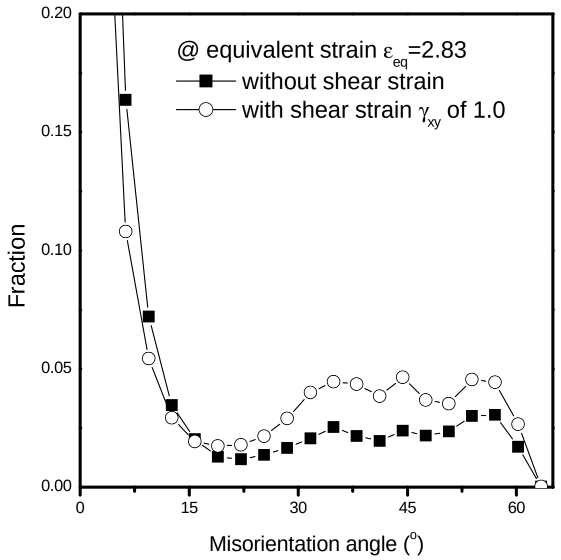

Fig. 7 One example of boundary misorientation distributions at equivalent plastic strain of 2.83 with and without shear strain of 1.0

HOME

excess of 30°. The LAGBs are plotted against the left vertical axis and all the HAGBs are plotted against the right in Fig. 8. As the equivalent strain increases, the fraction of HAGB (15°-30°) increases almost in the similar way regardless of the presence of shear strain. The fraction of HAGB (>30°) increases mainly at the expense of LAGB (<15°). Such the expense occurs at much higher rate with shear strain than without shear strain. Figure 9 represents the change of the fraction of grain boundary misorientation by γ_{xy} when ε_{eq} is 1.5. The fraction of HAGB (>30°) increases mainly at the expense of LAGB (<15°) with an increase in γ_{xy}.

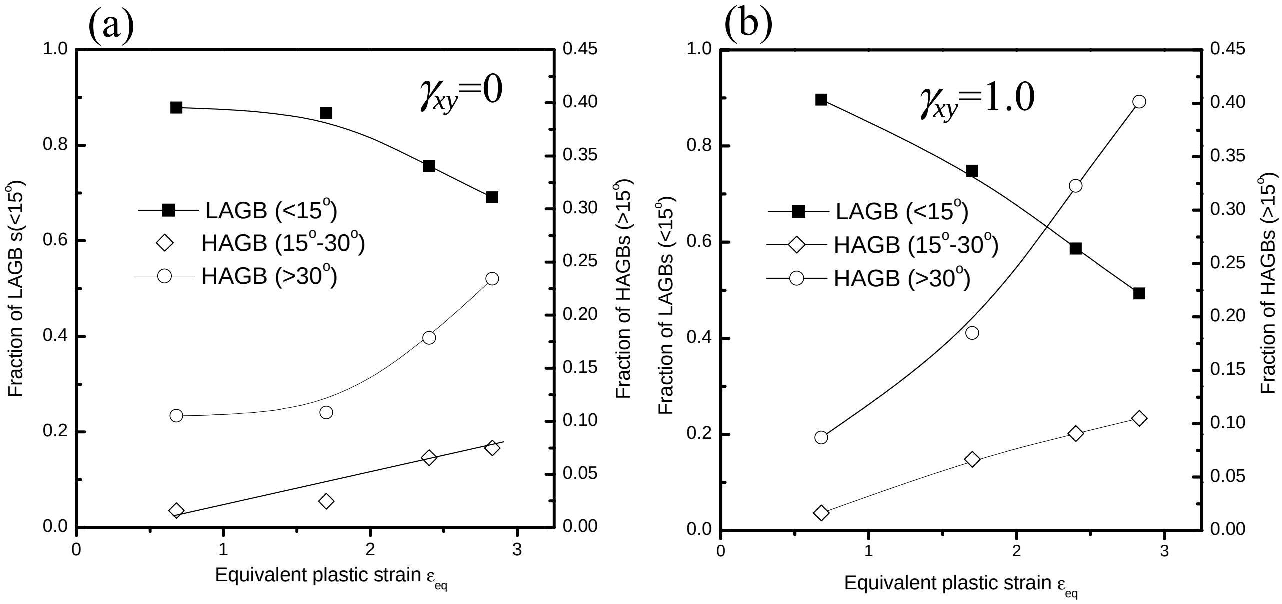

Fig. 8 Comparison of the rates of development of boundary area fractions according to equivalent plastic strains (a) without and (b) with shear strain of 1.0.

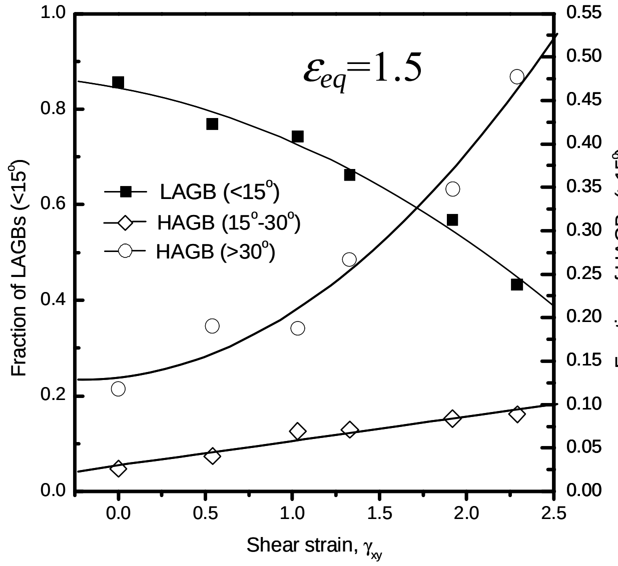

Fig. 9 Rates of development of boundary area fractions according to shear strains at ε_{eq}=1.5

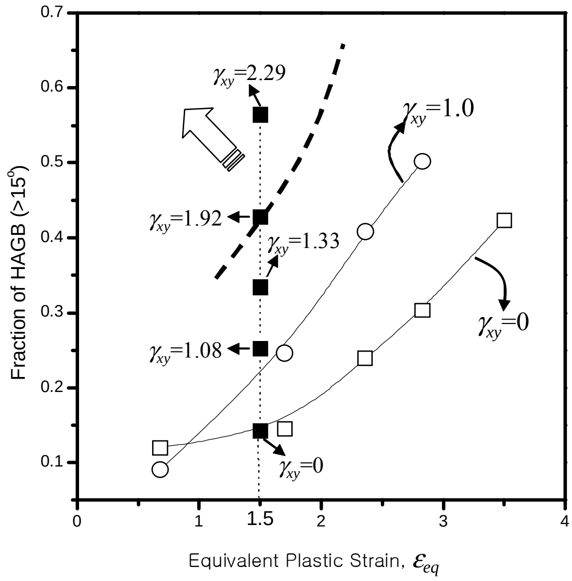

Fig. 10 Effect of shear strain on fraction of HAGB area, plotted as a function of equivalent strain

HOME

Figure 10 represents the fractions of HAGB area according to shear strain, with fixing the equivalent strain at ε_{eq}=1.5, together with the data of Fig. 6. It is likely that the curve passing through the point indicated by γ_{xy}=1.92 might follow the dotted bold line with increasing ε_{eq}. And the curves will move in the upper left-handed direction with an increase of shear strain component, as indicated by the arrow in Fig. 10. Hence, it is implied that the same HAGB fraction can be reached much rapidly at a relatively small equivalent strain, with increasing the shear strain component.

4. CONCLUSIONS

On the basis of the calculated strain distribution induced by hot compression, the microstructural evolution behaviors in the positions with and without the shear strain were compared. The results are as follows.

(1) The fraction of high angle grain boundaries (HAGBs) with misorientations over 15^o increases with an increase in the equivalent strain. Such the expense occurs at much higher rate with shear strain than without shear strain.

(2) Even if the equivalent strain is the same, the fraction of HAGBs with misorientations over 15^o increases with an increase in the shear strain, especially the fraction of HAGBs over 30^o increases at much higher rate.

(3) The shear strain component is more effective to develop HAGBs in austenite grain interiors than the compressive strain.

REFERENCES

1) J.G. SEVILLANO, P.Van HOUTTE and E. AERNOUDT, Prog. Mater. Sci. 25, (1980), p. 69.
2) T. INOUE, S. TORIZUKA, K. NAGAI, K. TSUZAKI and T.OHASHI, Mater. Sci. Tech. 17, (2001), p.1580.
3) T. INOUE, S. TORIZUKA and K. NAGAI, Mater. Sci. Tech. 18, (2002), p.1007.
4) P.J. HURLEY, B.C. MUDDLE and P.D. HODGSON, Metall. Mater. Trans. 32A, (2001), p.1507.